Crystallization Mechanism of Syndiotactic Polypropylene Analyzed by Time-Dependent Light Scattering

T. Kawai* and G. Strobl

Physikalisches Institut, Albert-Ludwigs-Universität Freiburg, 79104 Freiburg, Germany

Received November 24, 2003; Revised Manuscript Received January 19, 2004

ABSTRACT: Monitoring the time dependence of polarized (vv) and depolarized (hv) light scattering during the crystallization of a polymer can be used to characterize the development of the size and internal structure of the growing spherulites or hedrites. In particular, it is possible to distinguish between a growth of objects with a fixed inner structure and cases of a subsequent inner structure modification. We report here on the crystallization of a sample of syndiotactic polypropylene from the melt. The vv- and hv-scattering patterns are indicative for the growth of hedrites and enable a specific direct evaluation procedure to be applied. We determined for several crystallization temperatures the final size of the hedrites, the crystallization time and observed, in particular, changes with time in the mean inner anisotropy and density. Observations speak in favor of an in-filling process of crystalline lamellae accompanying the hedrite's growth. From a complementary dilatometric determination of the specific volume change and its agreement with kinetical data of the light-scattering experiments it follows that the number of growing hedrites is constant.

1. Introduction

In many works on polymer crystallization, measured crystallization isotherms are represented using the Avrami equation. Such a treatment implies the assumption that polymer crystallization proceeds by the growth of objects—spherulites or hedrites—with a fixed, well-defined inner structure. This, however, is not generally the case, as one often encounters a sequential building-up of the inner structure which goes on within the growing objects.

Different mechanisms are discussed in the literature as causing a continuous inner structure formation. In electron microscopic investigations, Bassett and Patel found evidence that objects can first develop as an open structure erected by some "dominant" lamellar crystallites, which is then followed by a filling-in of subsidiary crystallites.[1] AFM real-time studies by Li et al.[2] and also time-dependent synchrotron-radiation microbeam experiments by Riekel et al.[3] corroborate such a sequential building-up. In recent time another possible cause is also discussed. There are several observations—in particular in IR spectroscopic and X-ray time-dependent investigations—which indicate a multistep route in polymer crystallization with a passage through transient states (compare[4] for a summary). This could also result in time-dependent changes in the inner object structure.

If the objects are sufficiently large, with sizes in the 10 μm range, subsequent inner structure formation processes can be observed directly in the polarizing microscope. The contrast of the objects is then found to increase with time and there exist even cases—for example, in copolymerized polyethylenes[5]—where no growth at all is observed, but just an increase in contrast within a geometrically invariant structure. Such a direct observation is no longer possible, if the objects are too small to be resolved in the microscope. In addition, it is difficult to use the contrast in micrographs in quantitative evaluations. Light-scattering experiments are the tool of choice to overcome these shortcomings; they provide quantitative data at higher resolution. By discriminating between time-dependent changes associated with the growth and the inner structure of objects respectively, they yield also another kind of information than the techniques usually employed in crystallization kinetical studies—time-dependent DSC , density, or X-ray scattering measurements. So far, compared to the other techniques, light scattering is seldom used. The data evaluation is considered to be difficult, and limitations exist due to the change in the sample transparency on crystallization. There are, however, favorable cases, and in this paper, we present one with a crystallizing syndiotactic polypropylene (sPP). For the final crystallinity below 30% reached here, the sample retains a sufficiently high transparency. Furthermore, the growing objects here are hedrites which produce an essentially isotropic scattering pattern, and this enables a direct evaluation procedure to be applied.

Much is already known about the structure of semicrystalline sPP. Morphological studies showed that sPP forms both hedrites and spherulites, depending on the crystallization temperature T_c (compare, e.g., refs 6−8). At high T_cs one finds hedrites and often also single crystallike objects with a rectangular, lath-shaped habit. For lower T_cs, an increasing tendency of branching and splaying of growing lamellae continuously changes the hedrites into spherulites. The crystal structure has been analyzed in detail. Since the early work of Natta and Corradini[9] it is known that the chain conformation corresponds to a t_2g_2 sequence for each syndiotactic repeating unit, setting up a helix with two syndiotactic units per turn with a period of 0.74 nm. The stable structure of sPP (modification III) has a unit cell which includes two left- and two right-handed helices in a regular alteration along both the *a* and the *b* axis (space group *Ibca*). In real crystals, the regular left-right packing is often perturbed, leading to lattice disorder. This disorder is known to increase with decreasing T_c.[10] We had carried out a comprehensive study of the

* Corresponding author.

10.1021/ma035759k CCC: $27.50
Published on Web 02/24/2004

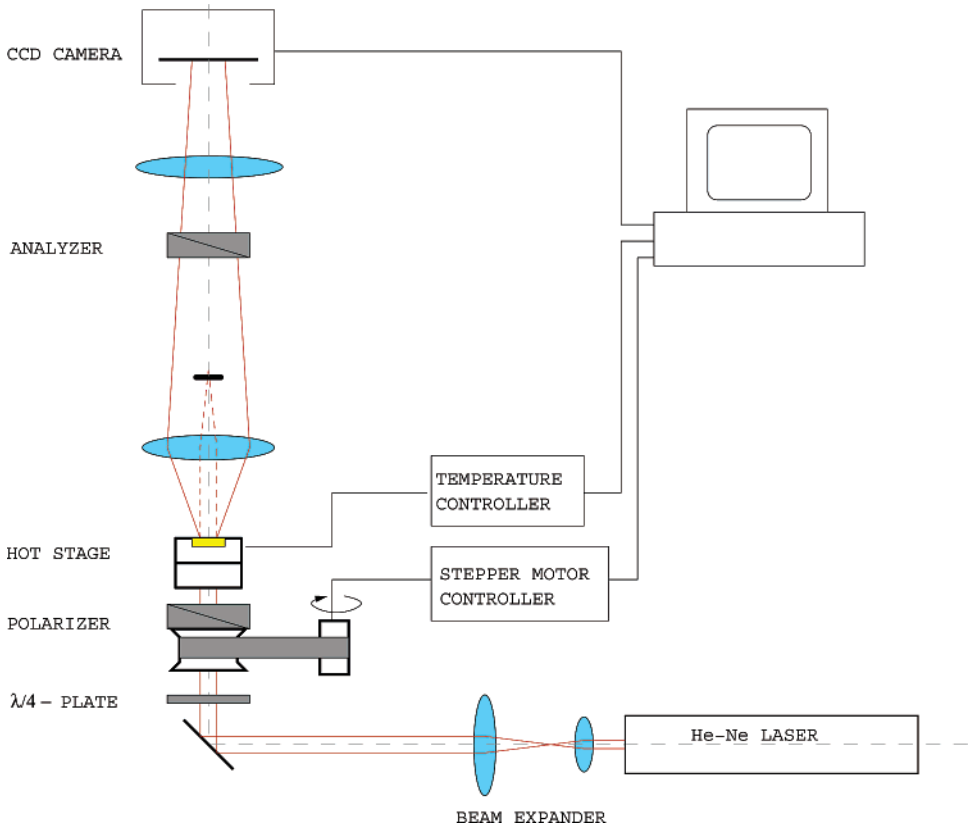

Figure 1. Setup of the light-scattering apparatus used for a simultaneous registration of vv- and hv-scattering curves.

lamellar structure formed at different crystallization temperatures for samples of different tacticity and (octene-)counit content.[11,12] It was therefore quite natural to use one of the samples now also in a light-scattering study of the crystallization process. The results are described in the following. They include a complementary time-dependent dilatometric measurement by which we could check some of the light-scattering results and decide about the possible occurrence of retarded homogeneous nucleation processes.

2. Experimental Section

2.1. Samples. sPP with 92% of syndiotactic diads, provided by Mitsui Chemical Co., Ltd., was used in this study without any further purification. sPP pellets were first dried under vacuum conditions at 110 °C for 12 h. A film sample with 100 μm thickness was then prepared by pressing the pellets between Teflon sheets at 180 °C, followed by quenching into ice water. The samples were covered by two glass plates, and then inserted into the hot stage in the scattering device and again melted at 180 °C for 20 min, followed by a cooling to the various crystallization temperatures. Since the temperature of 180 °C is well above the equilibrium melting point reported for a similar sample $T_f^\infty = 160$ °C,[12] it can be assumed that the crystallization starts from a relaxed equilibrated melt.[13]

2.2. Light-Scattering Camera. Simultaneous polarized and depolarized light-scattering measurements were carried out with a home-built apparatus. The optical setup is described in Figure 1, and the scattering geometry is shown in Figure 2. A He−Ne laser beam ($\lambda = 633$ nm) is expanded to cover a larger sample area. Using a polarizer that can be rotated by a stepping motor makes it possible to register simultaneously both hv- (polarizer perpendicular to analyzer) and vv-scattering patterns (polarizer parallel to analyzer). The scattering patterns were registered by a CCD camera with 769 × 512 pixels on an area of 6.9 × 4.2 mm^2. A PC collects all data and

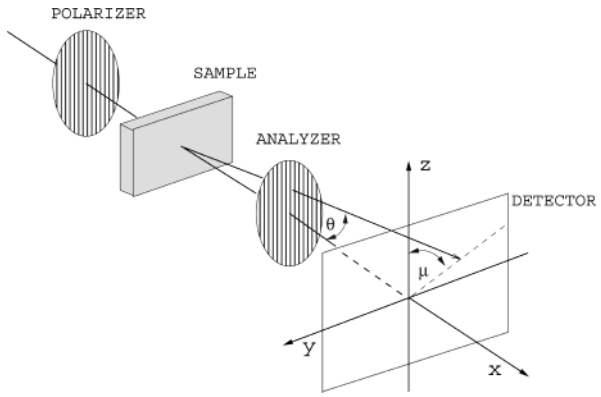

Figure 2. Scattering geometry. Scattered light is registered in the q_y,q_z plane, keeping the analyzer direction fixed along z. The incident laser beam which propagates along x is either z- (for vv-) or y-polarized (for hv-scattering).

was also used for the further analysis of the scattering intensity distribution.

2.3. Dilatometry. Complementing the light-scattering experiments, density changes during the isothermal crystallization of sPP were investigated by dilatometry. A sample of 125 mg sPP was inserted into the dilatometer followed by an evacuation at melt temperatures. Then mercury was added to fill the dilatometer. Two oil baths were used for the measurement. The dilatometer was first put in an oil bath for 20 min at a temperature of 180 °C and then quickly moved into another oil bath which was preheated to various crystallization temperatures in the range from 103 to 125 °C. The changes of the volume during the crystallization were recorded at discrete times.

3. Analysis of the Light-Scattering Patterns

We used a direct approach which is applicable for hedrites with a uniform chain orientation. Applying a

general relation to the case of hv-light-scattering with an intensity distribution $I^{hv}(q_x, q_y, q_z)$ (q_x, q_y, q_z are the components of the scattering vector with $q = 4\pi(\sin\theta)/\lambda$, θ denoting the Bragg angle), the mean squared optical anisotropy as expressed by the *yz* component of the polarizability tensor, $\langle(\alpha_{yz})^2\rangle$, can be related to the integral scattering intensity, denoted as Q_3^{hv}, by the equation

$$\langle(\alpha_{yz})^2\rangle \sim \int I^{hv}(q_x, q_y, q_z)\, dq_x\, dq_y\, dq_z = Q_3^{hv} \quad (1)$$

If no correlation exists between the orientation of different hedrites and if these objects occupy at a certain stage of the development a fraction ϕ of the volume, we can write

$$\langle(\alpha_{yz})^2\rangle = \phi\,\overline{(\alpha_{yz})^2} \quad (2)$$

The overline denotes the average over all orientations of the hedrites. When the sample is completely covered with hedrites, i.e., $\phi = 1$, Q_3^{hv} is a direct measure for the objects' inner anisotropy as expressed by $\overline{(\alpha_{yz})^2}$. For *n* objects per unit volume, the volume fraction ϕ occupied by them can be written as

$$\phi \simeq n l_h^3 \quad (3)$$

where l_h denotes the dimension of the hedrites. This leads for the integral scattering intensity to

$$Q_3^{hv} \sim n l_h^3 \overline{(\alpha_{yz})^2} \quad (4)$$

A second parameter of interest is the forward scattering $I_0^{hv} = I^{hv}(q \to 0)$. As will be shown, it could be directly determined in our experiments. For a random orientational distribution without any correlation between neighboring objects, I_0 follows by an addition of the intensities of all objects, as

$$I_0^{hv} \sim n\,(\int_{obj} \alpha_{yz}\, d^3\mathbf{r})^2 \quad (5)$$

$$\simeq n l_h^6 \overline{(\alpha_{yz})^2} \quad (6)$$

When the crystallization proceeds as usual after a heterogeneous nucleation, i.e., with n = const, one expects, according to eqs 4 and 6 for an assumed linear increase of the object diameter with time, an increase of Q_3^{hv} and I_0^{hv} during the initial stages with power laws

$$Q_3^{hv} \sim t^3, \quad I_0^{hv} \sim t^6 \quad (7)$$

It is also possible to derive information from vv-scattering. The integral over the intensity distribution of polarized scattering $I^{vv}(q_x, q_y, q_z)$ is determined by the mean squared fluctuation of the *zz*-component of the polarizability, $\delta\alpha_{zz}$ ($\delta\alpha_{zz}$ denotes the difference to the polarizability of the melt), as

$$\langle\delta\alpha_{zz}^2\rangle - \langle\delta\alpha_{zz}\rangle^2 = \int I^{vv}(q_x, q_y, q_z)\, dq_x\, dq_y\, dq_z \sim Q_3^{vv} \quad (8)$$

The fluctuation term can be written as

$$\langle\delta\alpha_{zz}^2\rangle - \langle\delta\alpha_{zz}\rangle^2 = \phi(1-\phi)(\delta\alpha^{is})^2 + \phi\overline{(\delta\alpha_{zz}^{an})^2} \quad (9)$$

The right-hand side of this equation is composed of two contributions. The first term refers to the density fluctuation in a two-phase structure with a density difference corresponding to $\delta\alpha^{is}$. With increasing volume fraction ϕ of the hedrites, this term passes over a maximum. The second term in eq 9 refers to the birefringence-related part of $\delta\alpha_{zz}$, written $\delta\alpha_{zz}^{an}$. It has the same form as that for α_{yz} in eq 2. When the sample is completely covered with objects, i.e., $\phi = 1$, only the anisotropic part remains:

$$Q_3^{vv} \sim \overline{(\delta\alpha_{zz}^{an})^2} \quad (10)$$

Hence, in both cases, hv- and vv-scattering, one can derive from the final integral scattering intensities the values reached by the anisotropy within the objects. Moreover, it is possible to derive from the maximum value of Q_3^{vv} which is reached for $\phi = 0.5$ the density difference $\delta\alpha^{is}$ (neglecting the much smaller contribution of the anisotropy scattering).

For the polarized forward scattering I_0^{vv} we formulate only a relation for the initial stages of the development. In analogy to eq 6, we can write

$$I_0^{vv} \simeq n l_h^6 (\delta\alpha^{is})^2 \quad (11)$$

neglecting again the much smaller contribution from $\delta\alpha_{zz}^{an}$.

4. Results

4.1. Light-Scattering Measurements. As is well-known, four-leaf clover patterns appear in the hv-mode when polymers crystallize as spherulites. Contrasting this behavior, all specimen in this study showed essentially circular symmetric scattering patterns, in both hv- and vv-modes. There was, if any, no appreciable azimuthal angle dependence, and the scattering intensity decreased monotonically from $q = 0$ without an intensity maximum at a certain angle. This shows that, confirming the general knowledge, for the chosen temperatures with low crystallization rates sPP forms hedrites rather than spherulites.

We found that for all the measurements the scattering curves were well represented by the Debye−Bueche function

$$I(q) = \frac{I_0}{(1 + l^2q^2)^2} \quad (12)$$

Here, I_0 is the scattering intensity in forward direction, and l is the correlation length of the associated two phase structure. In the Debye−Buche plot, where $I^{-1/2}$ is plotted against q^2, the value at zero angle and the slope yield I_0 and $l^2/I_0^{-1/2}$, respectively. Figure 3 shows typical results for Debye−Bueche plots of the scattering intensity measured at various times during an isothermal crystallization at 118 °C. In both hv- and vv-scattering, the plots produce only weakly curved lines. Linear extrapolations of the initial sections near to the origin enable I_0 and l to be obtained with an accuracy of at least ±10%.

Since the scattering intensity distribution is essentially isotropic, one can also estimate the integral scattering intensity in reciprocal space, Q_3, for both vv-

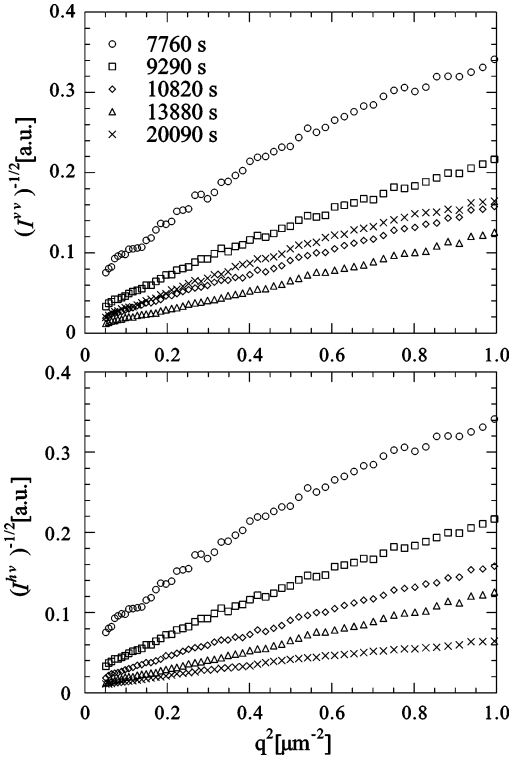

Figure 3. sPP, crystallized at T_c = 118 °C: vv(upper part) and hv(lower part) light-scattering curves measured at the indicated times, represented according to the Debye−Bueche structure function.

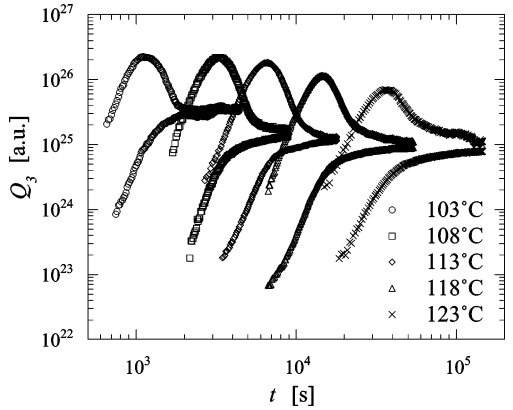

Figure 4. Change of the integral scattering intensities Q_3^{vv} (open symbols) and Q_3^{hv} (filled symbols) during the crystallization at various T_cs.

and hv-scattering, by using the relation

$$Q_3 = \frac{\pi^2 I_0}{l^3} \tag{13}$$

valid for the Debye−Bueche structure factor. We will discuss the crystallization of sPP by using three different parameters, namely the forward scattering intensity I_0, the correlation length l and the integral scattering intensity Q_3 for both vv- and hv-scattering.

Figure 4 shows the time evolution of Q_3 crystallized at various temperatures. At the early stages of crystallization both Q_3^{hv} and Q_3^{vv} show a continuous increase with time. Q_3^{hv} keeps a steady increase until the end, while Q_3^{vv} passes over a maximum and then ends up at a similar level as Q_3^{hv}. This comes as expected consid-

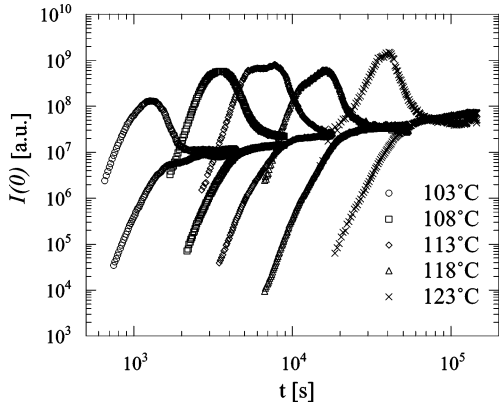

Figure 5. Time dependence of vv- and hv-scattering intensity in forward direction, I_0^{vv} (open symbols) and I_0^{hv} (filled symbols), during the crystallization at various T_cs.

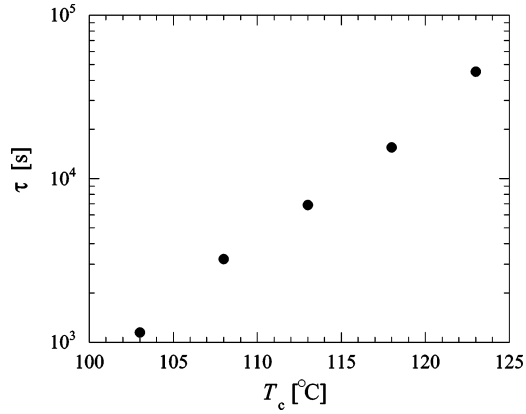

Figure 6. Variation of the crystallization time as a function of the crystallization temperature T_c.

ering eqs 1, 2, 8, and 10. The final values of Q_3 for both hv- and vv-scattering are directly related to the anisotropy within the objects as expressed by the components α_{yz} and $\delta\alpha_{zz}^{an}$.

Figure 5 represents the variation with time of I_0 at various crystallization temperatures T_c. It can be seen that, as in $Q_3(t)$, the time required for the crystallization increases systematically with T_c. The crystallization times τ, here derived from the points of intersection of the initial and final linear parts in the log−log-plots in Figure 5, are plotted against T_c in Figure 6. For a given T_c, a steady increase in intensity is observed in the early stage of crystallization for both I_0^{hv} and I_0^{vv}. This continues for I_0^{hv} until the end, while I_0^{vv}—similar to Q_3^{vv}—passes over a maximum.

For the usual case of a heterogeneous nucleation, i.e., n = const, and constant linear growth rates one expects from eqs 4, 6, and 11 for both vv- and hv-scattering initial power laws $Q_3 \sim t^3$ and $I_0 \sim t$.[6] Our observation, however, shows a proportionality to t^ν with $\nu = 9 \pm 0.3$ for I_0^{hv}, I_0^{vv} and $Q_3^{vv} \sim Q_3^{hv} \sim t^\mu$ with $\mu = 6 \pm 0.3$.

From the Debye−Bueche plots in Figure 3, we can derive the correlation lengths l^{hv} and l^{vv}. The correlation length l^{hv} provides for all times a measure for the size of the hedrites, i.e., eqs 4 and 6 can be used with $l_h = l^{hv}$. The correlation length derived from the vv-scattering curve, l^{vv}, does not always give the hedrite size. It can be representative for either the hedrites or the melt-filled holes between them, depending on the degree of filling (see ref 14 for more details). Figure 7 shows the time development of the correlation lengths during the

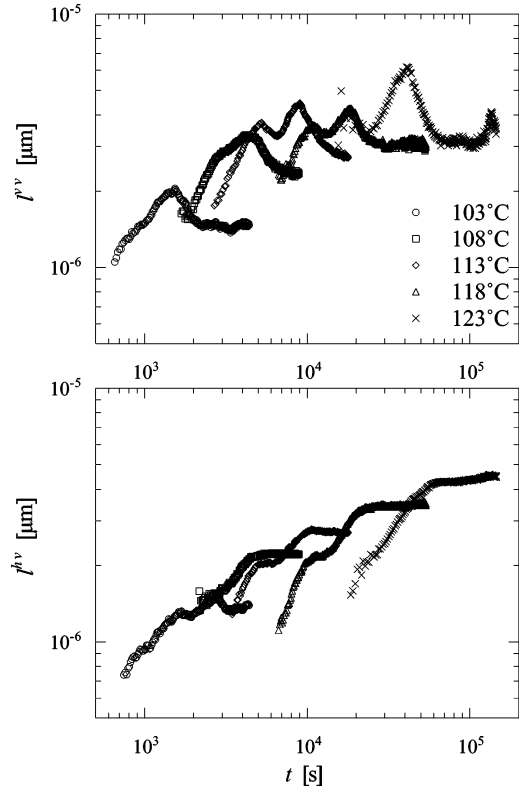

Figure 7. Development with time of the correlation lengths l^{vv} (top) and l^{hv} (bottom) derived from Debye−Bueche plots, measured at various T_cs.

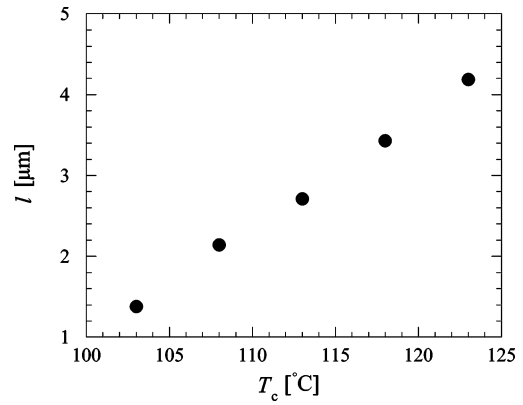

Figure 8. Change of the diameter of the final objects as given by l^{hv} with T_c.

crystallization at various T_c. At the early stage of crystallization, l^{hv} and l^{vv} show a steady increase with time due to the increase of the object size. Then fluctuations are observed in the time dependence, which comes as expected for l^{vv}, but is found also for l^{hv}. The latter observation indicates that the orientation of crystals is not ideally random; obviously some orientational correlation exists between neighbors. This is, however, conceivable in view of the planar form of hedrites.

One can see clearly an increase in the final values of l^{hv} and l^{vv} with increasing T_c. The final value of l^{hv} giving the size of the hedrites at the end of the crystallization is plotted in Figure 8.

We have to check the attenuation changes during the crystallization because the scattering intensity can be much affected by the varying light transmittance of the sample. Figure 9 shows the change in the transmitted

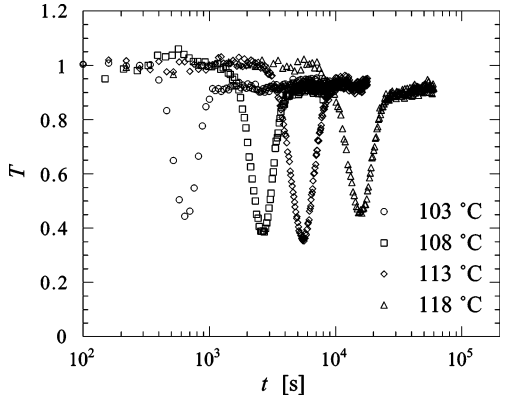

Figure 9. Change in the transmitted laser beam intensity during the crystallization at various T_cs.

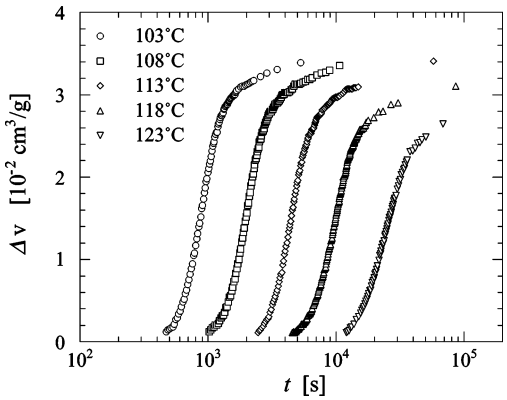

Figure 10. Change in the specific volume during the crystallization at various T_cs observed in dilatometric measurements.

light intensity of the laser beam during the crystallization at various T_cs in plots of the relative intensity $I(t)/I(0)$ against time; $I(0)$ means the transmitted light intensity at $t = 0$. One has a stronger attenuation at the half-time of crystallization, but a constant high value of transmission of 0.9 at the end. The final value as well as the minimum value do not depend on T_c. We did not make an attempt to correct the measured data for the attenuation, because this still would not provide results which can be directly interpreted. For stronger attenuations, say above 20%, multiple scattering can no longer be neglected. Fortunately our main conclusions refer to the initial stages of development and the final structure, and here the attenuation remains small or moderate.

4.2. Dilatometry. For specific comparisons with light-scattering results we also carried out dilatometric measurements of the crystallization under isothermal conditions, again at various T_cs. Figure 10 shows the crystallization isotherms obtained. The variation with time of the change of the specific volume, $\Delta v(t)$, for various T_c is presented. The volume change during the crystallization can be written as

$$\Delta v(t) = v(0) - v(t) \sim \phi \Delta v_{obj} \qquad (14)$$

Here, ϕ is the volume fraction of the objects within the sample, and Δv_{obj} denotes the difference in the specific volume between melt and object.

For lower T_cs, the shape of the curves is constant. Above $T_c = 113$ °C, the final value gradually decreases with increasing T_c.

5. Discussion

What could be the reason for the unusually high exponent in the initial power law

$$I_0^{hv} \sim I_0^{vv} \sim t^9 \tag{15}$$

found for the forward scattering intensity? Figure 8 indicates for the object size as given by l^{vv} or l^{hv} at 123 °C during the initial stages a linear increase with time (for lower temperatures, where the number density of hedrites is higher, orientational correlations arise, which modify the curves $l^{hv}(t)$). One therefore might expect, at first

$$I_0 \sim l^6 \sim t^6 \tag{16}$$

for both vv- and hv-scattering which, however, differs from the observation. On the basis of eqs 6 and 11, we must conclude that the mean density and anisotropy as reflected in the values of $(\delta\alpha^{is})^2$ and $\overline{\alpha_{yz}^2}$ are not constants, but increase during the growth of the hedrites according to the law

$$(\delta\alpha^{is})^2 \sim \overline{\alpha_{yz}^2} \sim t^3 \tag{17}$$

A look at both Figures 4 and 7 shows also that this change of the inner structure even continues when the hedrites have already reached their final size. Hence, we encounter for this sample a sequential building-up of the object's inner structure. In the introduction two different possible causes were given, a subsequent filling-in of subsidiary crystals into the primary construction of dominant crystals, or the passage through a transient phase. The fact that the mean density $(\delta\alpha^{is})^2$ and the mean anisotropy $\overline{\alpha_y^{22}}$increase together in strict proportionality speaks in favor of the first mechanism, i.e., an ongoing filling-in process.

We can draw these conclusions only if the number of growing objects is constant, since an increase of n would also affect the exponent in the initial power laws for I_0. This is usually the case but—to be sure—can also be checked by the dilatometric measurement. Of interest is here a comparison of the kinetics of volume change with the time dependence $I_0^{hv}(t)$ on the following basis: For a constant number density n of growing hedrites there is

$$\Delta v(t) = n l(t)^3 \delta v(t) \tag{18}$$

where l^3 denotes the hedrite volume and δv the difference between the specific volume of the melt and the mean specific volume of a hedrite. Referring to the depolarized light scattering, we have for a constant n according to eq 6

$$I_0^{hv}(t) \sim n(l^{hv}(t))^6 \overline{(\alpha_{yz}^2)}(t) \tag{19}$$

and therefore

$$(nI_0^{hv}(t))^{1/2} \sim n(l^{hv}(t))^3 \overline{(\alpha_{yz}^2)}^{1/2}(t) \tag{20}$$

n can be derived from the final hedrite volume, as

$$n \simeq (l^{hv}(t \to \infty))^{-3} \tag{21}$$

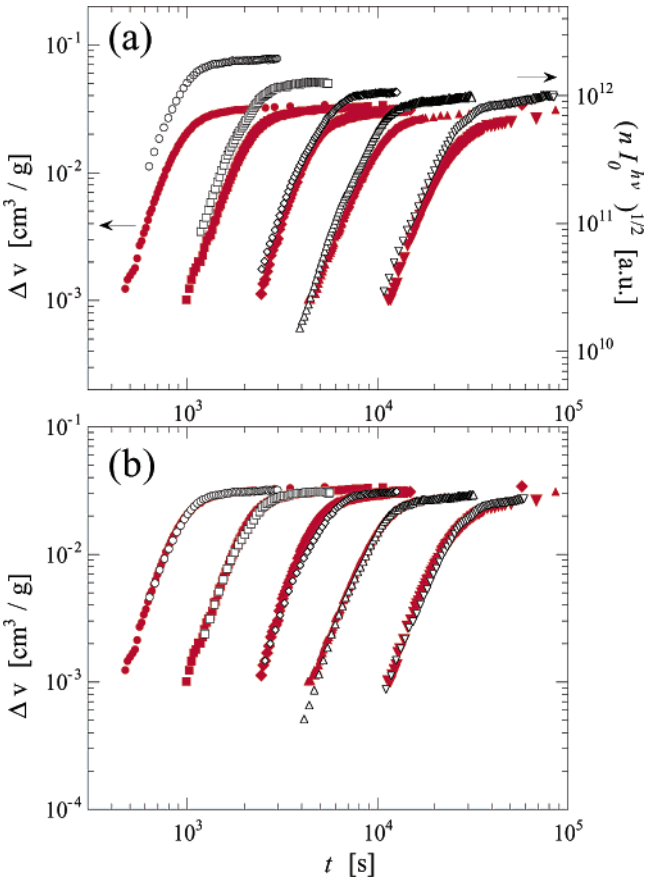

Figure 11. Comparison of the results of dilatometric ($\Delta v(t)$) and hv-light-scattering measurements ($(nI_0^{hv})^{1/2}$) during isothermal crystallizations: (a) direct results showing a different T_c dependence of the final values; (b) adjustment of the light-scattering curves demonstrating the equivalence of the registered kinetics.

Figure 11 presents at the top (a) a comparison of $\Delta v(t)$ with the property given by expression 20. The light-scattering results were shifted by a factor 1.5 along the log t axis to account for a derivation of 2 °C of the nominal from the true temperature in the sample holder. As it appears, the shapes of the kinetical curves obtained by dilatometry and anisotropic light scattering are identical. For the direct check, the curves derived from $I^{hv}(t)$ were individually shifted in vertical direction until a maximum overlap. The results are given in the bottom figure, and they demonstrate a perfect equivalence.

This finding of an equal kinetics of the specific volume and the property in eq 20 derived from anisotropic light scattering implies the following:

- A strict proportionality between $\overline{(\alpha_{yz}^2)}^{1/2}(t)$ and $\delta v(t)$, i.e., of the mean anisotropy and mean density of the hedrite, holds throughout the whole period of development.
- The number n is indeed a constant; i.e., no retarded homogeneous nucleation after the primary hetergeneous nucleation occurs.

Although the ratio between the mean density and the mean anisotropy is thus constant during a crystallization, it changes between different T_cs. Figure 11a indicates a remarkable drop of the final value of the inner anisotropy between 103 and 113 °C, while the final Δv values remain here essentially constant. A decrease in the final values of Δv then follows for the

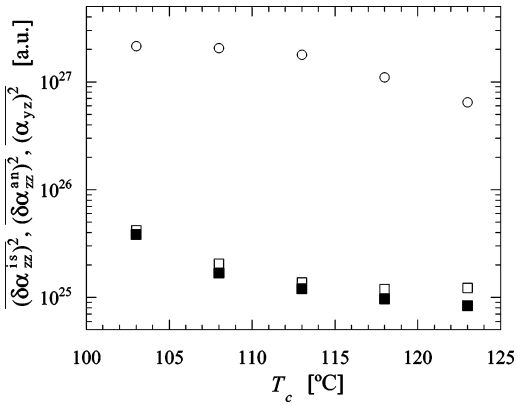

Figure 12. Change of the final values of $\overline{(\delta\alpha_{zz}^{is})^2}$ (circle), $\overline{(\delta\alpha_{zz}^{an})^2}$ (square), and $\overline{(\alpha_{yz})^2}$ (filled square) with T_c.

higher temperatures, 118 and 123 °C. This is again in agreement with the light-scattering results, now considering the maximum values of Q_3^{vv} in Figure 4. They also remain essentially constant up to $T_c = 113$ °C and then decrease. Figure 12 shows the values derived for the mean density and anisotropy of the hedrites, on the basis of the equations

$$Q_3^{hv}(\phi = 1) \sim \overline{\alpha_{yz}{}^2} \tag{22}$$

$$Q_3^{vv}(\phi = 1) \sim \overline{(\delta\alpha_{zz}^{an})^2} \tag{23}$$

$$Q_3^{hv}(\phi = 0.5) \sim \overline{(\delta\alpha^{is})^2} \tag{24}$$

The difference in the T_c dependence of the mean density and the anisotropy is obvious. The decrease of the quantities is indicative for a drop in the crystallinity, which does not come unexpected considering the stereoirregularity in the chains. Crystallite thicknesses increase with increasing T_c and the number of sufficiently long perfect sequences, which are required for the crystallites, then might become too small to further realize the basic, temperature-independent crystallinity found at the lower temperatures.[15]

Acknowledgment. The authors express their thanks to the Deutsche Forschungsgemeinschaft for the support of this work.

References and Notes

(1) Bassett, D. C.; Patel, D. *Polymer* **1994**, *35*, 1855.
(2) Li, L.; Chan, C.-M.; Yeung, K. L.; Li, J.-X.; Ng, K.-M.; Lei, Y. *Macromolecules* **2001**, *35*, 316.
(3) Kolb, R.; Wutz, C.; Striebeck, N.; von Krosigk, G.; Riekel, C. *Polymer* **2001**, *42*, 5257.
(4) Strobl, G. *Eur. Phys. J. E* **2000**, *3*, 165.
(5) Heck, B.; Strobl, G.; Grasruck, M. *Eur. Phys. J. E* **2003**, *11*, 117.
(6) Lovinger, A. J.; Davis, D. D.; Lotz, B. *Macromolecules* **1991**, *24*, 552.
(7) Rodriguez-Arnold, J.; Bu, Z.; Chen, S. Z. D.; Hsieh, E. T.; Johnson, T. W.; Geerts, R. G.; Palackal, S. G.; Hawley, G. R.; Welch, M. B. *Polymer* **1994**, *16*, 5194.
(8) Thomann, R.; Wang, C.; Kressler, J.; Jungling, S.; Mullhaupt, R. *Polymer* **1995**, *36*, 3795.
(9) Corradini, P.; Natta, G.; Ganis, P.; Temussi, P. *J. Polym. Sci., Part C* **1967**, *16*, 2477.
(10) Lovinger, A. J.; Lotz, B.; Davis, D. D.; Padden, F. J., Jr. *Macromolecules* **1993**, *26*, 3494.
(11) Hauser, G.; Schmidke, J.; Strobl, G. *Macromolecules* **1998**, *31*, 6250.
(12) Men, Y.; Strobl, G. *J. Macromol. Sci.—Phys.* **2001**, *B40*, 775.
(13) Supaphol, P.; Lin, J. *Polymer* **2001**, *42*, 9617.
(14) Hoffmann, A.; Strobl, G. *Polymer* **2003**, *44*, 5803.
(15) Heck, B.; Hugel, T.; Iijima, M.; Sadiku, E.; Strobl, G. *New J. Phys.* **1999**, *1*, 17.1.

MA035759K